

## Low-cost field goniometer for multiangular reflectance measurements

BEN LANDIS AND JAMES S. ABER -- *Earth Science Department, Emporia State University, Emporia, KS 66801. Corresponding author J.S. Aber (jaber@emporia.edu).*

A low-cost field goniometer was constructed for multiangular reflectance measurements using a spectral radiometer. The goniometer consists of a circular base made of plywood approximately 4 m in diameter. A rotating arch carries a sled with the radiometer, which can be positioned at any angle relative to the test object at the center of the goniometer. Data from the radiometer are downloaded to a portable computer via a serial cable. The goniometer was tested on a typical lawn, and spectral measurements were collected in the solar plane and at right angles to the solar plane. Spectral characteristics of the test lawn differed significantly from idea lawn grass. Maximum reflectance was measured at the antisolar point in visible light, but maximum infrared reflectance took place at a different position. These results demonstrate the value of collecting in-situ spectral data for evaluation of ground-cover conditions.

*Keywords: goniometer, remote sensing, spectral radiometer, antisolar point.*

### INTRODUCTION

Remote sensing is a means to collect information about objects from a distance. In the context of earth-resources remote sensing, various airborne and space-based instruments are utilized to acquire imagery and spectral information, such as aerial photographs, satellite imagery, and astronaut photography. Since the launch of the first Landsat satellite in 1972, remote sensing has become a fundamental method for documenting, mapping, analyzing, and understanding natural and cultural conditions worldwide (Lauer, Morain and Salomonson 1997). The number and types of remote-sensing systems have increased dramatically in recent years, operated by governmental agencies and commercial ventures (Jensen 2007). Among the most popular systems are those designed to acquire imagery in visible and infrared bands of the spectrum, so-called multispectral remote sensing.

Along with the rapid growth in remote sensing has come a need for improved knowledge of the spectral qualities of common objects on the Earth's surface—minerals, soil, water, vegetation, etc. This may be done under carefully controlled laboratory conditions, which simulate ideal solar illumination of test objects and measure reflectivity of those objects (Fig. 1). Such spectral signatures are quite useful; however, they do not correspond exactly to reflectivity of objects illuminated naturally. Nor do such laboratory spectral signatures match the type of data commonly acquired by remote-sensing instruments under routine operating conditions. To overcome these limitations, ground-based field collection of reflectance data is conducted with various hand-held or mounted spectral radiometers that are positioned within a few meters of test objects. The intent is to acquire spectral signatures for objects under natural conditions. Such measurements may be used to (Jensen 2007):

- determine spectral characteristics of selected materials.
- calibrate data collected from airborne or space-based remote sensing.
- improve analysis of multispectral remotely sensed data.

Most remote-sensing systems look straight down, acquiring vertical (nadir) or near-vertical views of the Earth's surface. During the past decade, several systems have been designed for collecting oblique or side views. Thus, a given object may be viewed from many directions, which gives rise to the complex phenomenon of multiangular reflectance, also known as bidirectional reflectance (Schönermark, Geiger and Röser 2004). To understand how light is scattered in the natural world is a difficult challenge for scientists and artists alike (Lucht 2004). To acquire multiangular reflectance measurements, goniometers have been built for both laboratory (Briottet et al. 2004) and field (Brugge et al. 2004) applications. The goal of this project was to build and operate a low-cost field goniometer for spectral radiometry.

### BIDIRECTIONAL REFLECTANCE

The phenomenon of bidirectional reflectance is the variation in reflectivity depending on the location of the sensor in relation to the ground target and sun position (Asner et al. 1998). The bidirectional reflectance distribution function (BRDF) refers to variations of reflectivity with different viewing angles, particularly within the solar plane. The solar plane is the vertical plane that contains the sun, ground target, and sensor (Fig. 2). The typical BRDF displays maximum reflectivity at the antisolar point, often called the hot spot or opposition effect, which is the position where the sensor is in direct alignment between the sun and the ground target. The cause of the hot spot is apparently the hiding of shadows at this position (Lynch and Livingston 1995; Hapke et al. 1996). The absence of visible

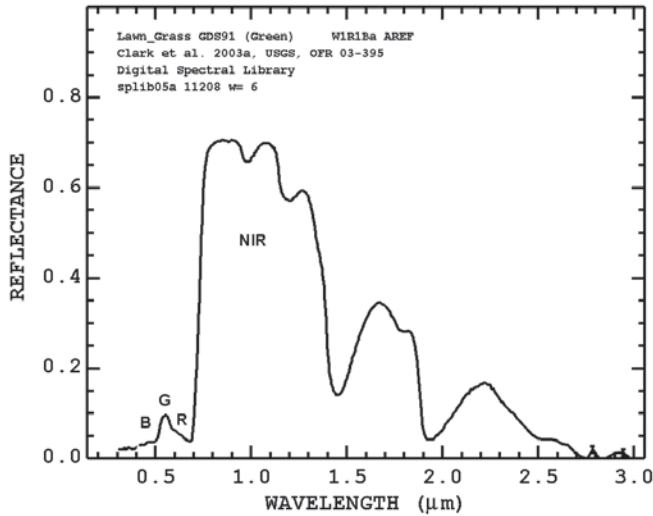


Figure 1. Spectral reflectivity for green lawn grass under laboratory conditions. Reflectance is given as a fraction of total illumination, as measured in a Nicolet spectrometer. Notice strong reflection in the near-infrared (NIR, 0.7-1.3 µm), weak reflection for green (G, 0.5-0.6 µm), and absorption of blue (B, 0.4-0.5 µm) and red (R, 0.6-0.7µm) light. This spectral pattern is unique to photosynthetically active vegetation. Adapted from Clark et al. (2003).

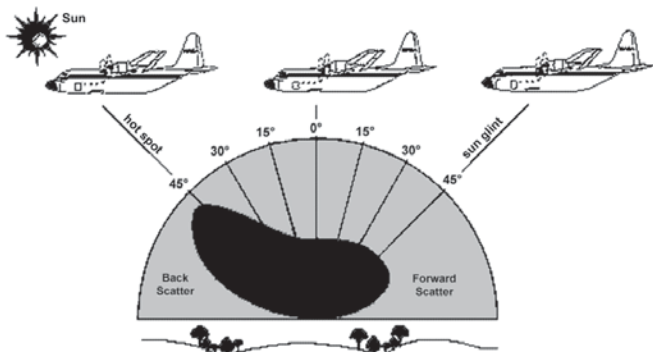


Figure 2. Diagram of aerial photography and typical BRDF. Amount of reflectivity in the solar plane is indicated by the black oval. Maximum reflectivity occurs directly back toward the sun. Illustration not to scale; adapted from Ranson, Irons and Williams (1994, fig. 1).

shadows causes the spot to appear substantially brighter than other views in which shadows appear (Fig. 3).

Considerable effort has been made to understand BRDF better for various types of land cover, particularly different vegetation canopies. One approach is to model mathematically the reflective plants and canopy geometry. Some models are based on radiative properties of plants (Nilson and Kuusk 1989), whereas others depend on geometric-optical considerations (Schaaf and Strahler 1994). In either approach, the models can be tested against actual sensor measurements, in others words ground truth collected with a field goniometer.



Figure 3. Hot spot displayed at the antisolar point in a harvested agricultural field. Note bright spot next to arrow (>). Kite aerial photograph, Poland (Aber and Gałazka 2000).

**GONIOMETER**

A typical goniometer consists of a horizontal circular frame, ~2 m in radius, with a vertical arch (Fig. 4). The arch carries a sled with the radiometer; the arch and sled can be moved into any position relative to the target at the center of observation. In this manner, spectral reflectance from the test object can be measured from all viewing angles around the hemisphere. Although simple in principle, construction of a functional goniometer involves several considerations. The ideal goniometer should be highly portable, consisting of relatively light-weight, robust, and small components. Furthermore it should be easy to set up quickly at a field site and require few people to operate. Finally, in our case, low overall cost of components and operation was a major design factor.

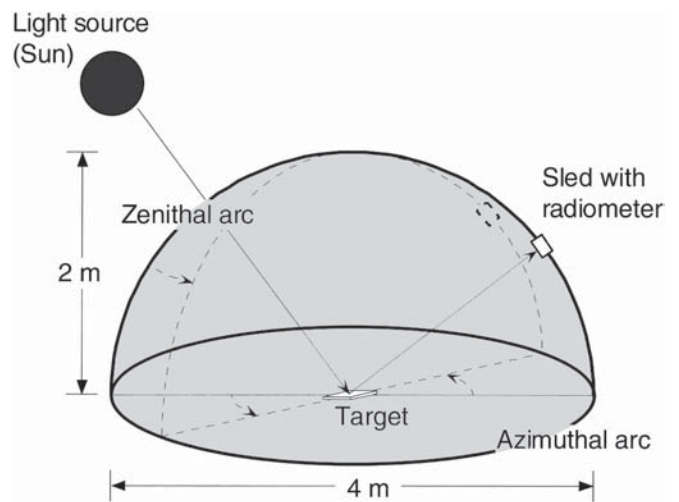


Figure 4. Schematic diagram of the field goniometer system (FIGOS) for multiangular, closeup measurement of reflectivity for targets under natural conditions. Adapted from Bruegge et al. (2004, fig. 5.10).

Our field goniometer approximates the size and structure of NASA's Sandmeier Field Goniometer (Ames 2007), which was patterned after the Swiss Field Goniometer (Bruegge et al. 2004). Building materials are conventional plywood, metal conduit, bolts and screws, steel plate, etc. The base consists of six pieces of plywood that fit together to form a full circle. Within the base, two circular tracks are cut to guide wheeled carriages that support the arch (Fig. 5). The arch is formed by steel conduit bent to the same curvature as the base. Two segments of arch are joined at the top by a "capstone" frame. The arch carries a small sled to which the radiometer is attached. The sled can be moved along the arch by means of a cord that runs over the capstone. Our existing spectroradiometer is a hand-held unit by Analytical Spectral Devices (Fig. 6). It is connected via serial cable to a portable computer for field operation. When fully assembled, the goniometer has a diameter slightly more than 4 m (Fig. 7).

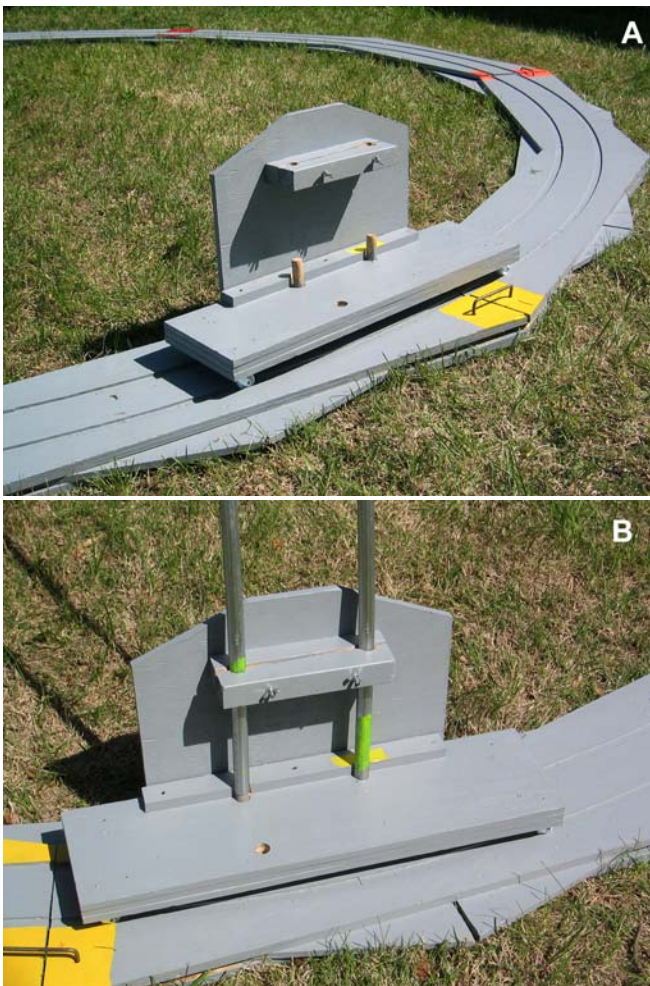


Figure 5. Detail of goniometer base and carriage for arch. A - segments of the base are color coded for correct assembly, and the carriage runs on two tracks cut into the base. B - carriage with conduit arch poles locked in place.

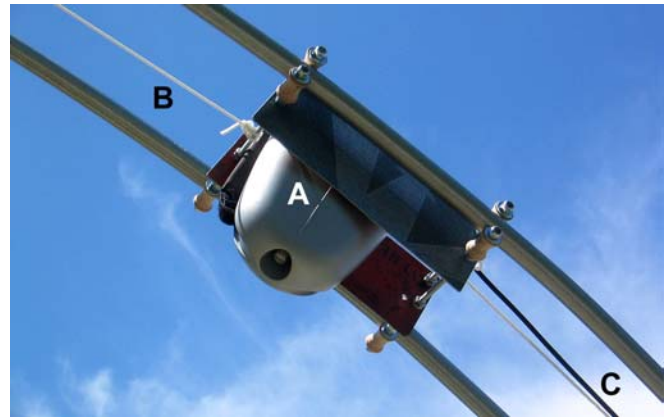


Figure 6. Detail of the sled on the arch. A - radiometer mounted in sled. B - cord to control sled position. C - serial cable to portable computer.



Figure 7. Fully assembled goniometer. Lead weights hold the arch carriages in their tracks. Shadows cast by the arch are minimal.

Building the goniometer involved considerable carpentry skills, and some minor difficulties were encountered. These were overcome through trial-and-error construction techniques. Total cost of goniometer materials was approximately \$250, not counting the radiometer and computer equipment.

The goniometer was assembled for a field test in late April on a typical mowed lawn consisting of fescue grass, dandelions, and patches of bare soil (Fig. 8). The test was conducted under full sun in late morning hours. The arch was placed in the solar plane, and measurements were taken at several positions toward and away from the sun. Then the arch was placed at right angles to the solar plane, and more measurements were collected at several positions. Finally vertical measurements were taken of the lawn as well as various other test objects. The entire process took approximately two hours.



Figure 8. Goniometer ready for field testing outside Science Hall on campus of Emporia State University. A portable computer is connected to the radiometer and is positioned under a nearby tree for shady operation.

#### SPECTRAL RESULTS AND INTERPRETATION

A typical spectral result for the lawn shows a large peak for green, reduced red, and another peak for near-infrared reflectance (Fig. 9). This response differs significantly from the ideal spectral signature for lawn grass (see Fig. 1). The ideal spectral signature has near-infrared reflectivity much higher than green, and reflectance of blue and red is minimal. The test lawn, in contrast, has green reflectivity slightly greater than near-infrared, and blue and red reflectance are significant also. The difference between the real lawn and ideal lawn grass may be explained by the presence of dead grass thatch and bare soil patches in the actual lawn. These materials are strongly reflective for visible light (Fig. 10), which increases the overall brightness in the visible portion of the spectrum.

In the solar plane, multiple measurements demonstrate maximum reflectivity at the antisolar point for green light (Fig. 11). However, for the near-infrared peak, the antisolar point is not the maximum value, which occurs at a backscatter position of  $-75^\circ$ . In general, reflectance for vertical and forward scatter (+) positions is less than for backscatter (-) positions in the visible portion of the spectrum (400-700 nm). Values are much closer together for infrared ( $>700$  nm) wavelengths, however. In the vertical plane at right angle to the solar plane, only slight differences are noted in reflectivity for multiple viewing positions (Fig. 12).

The spectral results in the solar plane for visible light conform to expectations that maximum reflectance is found at the antisolar position (Lynch and Livingston 1995). However, results in the infrared wavelengths show differences that may be attributed to vegetation microstructure. Reflectivity of vegetation is strongly anisotropic because of complex geometry of plant bodies and leaves. At the canopy level of the test lawn, variations in spectral properties, areas, and angles of leaves may influence infrared reflectivity in ways that are difficult to predict (Schaaf and Strahler 1994; Anser et al. 1998).

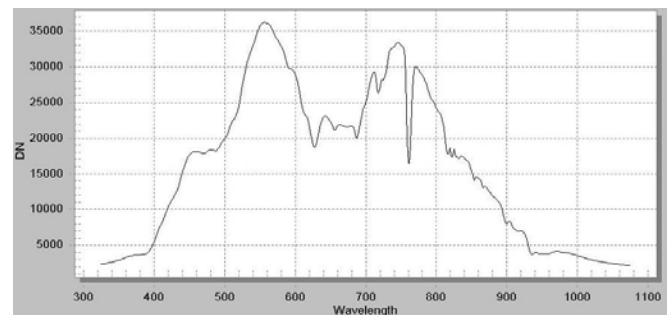


Figure 9. Spectral response curve for the test lawn as measured vertically using the goniometer. Wavelengths given in nanometers. Note green (500-600 nm) and near-infrared (700-800 nm) peaks, separated by a depression for red (600-700 nm) light. Compare with ideal lawn grass spectral signature (see Fig. 1).

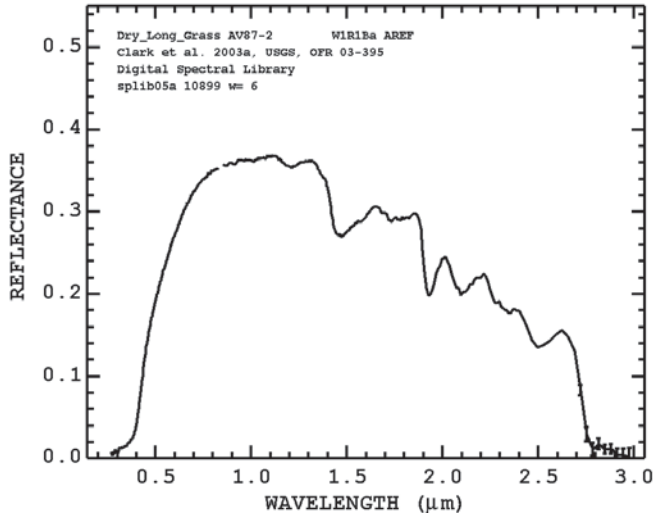


Figure 10. Spectral reflectivity for dry lawn grass under laboratory conditions. Reflectance is given as a fraction of total illumination, as measured in a Nicolet spectrometer. Notice strong reflections across all the visible (0.4-0.7 $\mu\text{m}$ ) and infrared (0.7-2.5  $\mu\text{m}$ ) portions of the spectrum. This pattern indicates the grass is dead. Taken from Clark et al. (2003).

#### ASSESSMENT OF GONIOMETER

The goniometer functioned successfully, which allowed us to acquire meaningful spectral data on reflectance of a test lawn under natural conditions of illumination. We achieved low cost with conventional building materials and volunteer labor to assist with construction of the device. The goniometer is reasonably easy to assemble, operate, and take down within a couple of hours. Based on our preliminary experience, three people should be sufficient for setup and operation of the goniometer.

The portable computer required shade in order to see the monitor effectively. A small tent or canopy would be desirable, or the person running the computer could sit in a shaded vehicle that also supplied power for extended computer operation. Transportation and storage of the goniometer are a bit awkward, because of the large size (8 feet long), weight, and odd shape of the base segments and long lengths of the arch segments. Nonetheless a full-sized pickup truck or cargo van would be adequate for transportation into the field.

#### CONCLUSIONS

A fully functional, low-cost field goniometer for spectral radiometry was designed and constructed patterned after NASA and Swiss goniometers. Results for a test lawn demonstrated significant differences compared with the spectral signature for ideal lawn grass. These differences may be attributed to the presence of dead grass thatch and bare soil patches in the test lawn, which increased visible reflectance

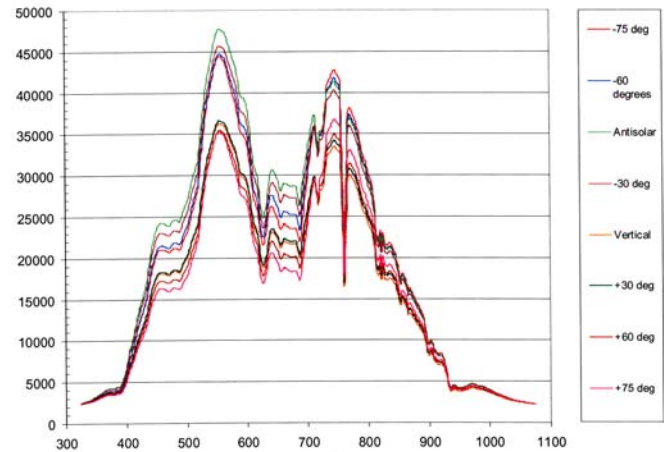


Figure 11. Composite chart of reflectivity in the solar plane for measurements at multiple positions using the goniometer. The bright green line indicates the antisolar point. Wavelengths given in nanometers.

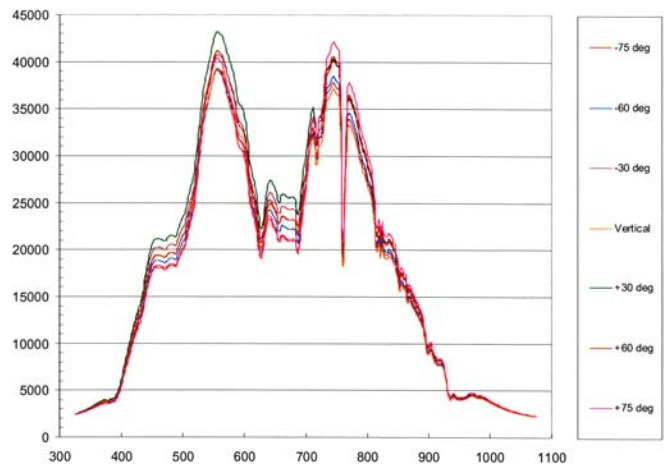


Figure 12. Composite chart of reflectivity at right angles to the solar plane for measurements at multiple positions using the goniometer. Wavelengths given in nanometers.

relative to infrared reflectance. Maximum reflectivity was measured at the antisolar point for visible light, as expected. However, the antisolar point was not the maximum value for infrared reflectance, presumably because of anisotropic characteristics of the lawn canopy. These results demonstrate the value of ground-based collection of in-situ spectral data for comparison with remotely sensed data from airborne and space-based instruments.

The goniometer could serve both educational and research purposes in the future. Its relatively simple setup and operation would be suitable for field demonstrations and student projects connected with courses in remote sensing. In addition, it would be valuable for continued research on multispectral reflectivity at the antisolar point for different kinds of ground cover.

## ACKNOWLEDGEMENTS

We thank J.M. Rioth for his help with design and construction of the goniometer; without his contribution this project would not have been possible. We also thank those who volunteered to help build and test the goniometer: J.M. Rioth, M. Davies, A. Landis, and L. Landis. Financial support was provided by grants from KansasView and Kansas NASA EPSCoR.

## REFERENCES

- Aber, J.S. and Gałazka, D. 2000. Potential of kite aerial photography for Quaternary research in Poland. *Geological Quarterly* 44, p. 33-38.
- Ames 2007. Ames technology capabilities and facilities: Instrument development. NASA Ames Research Center. Access online, July 2007 <[http://www.nasa.gov/centers/ames/research/technology-onepaggers/instrument\\_development.html](http://www.nasa.gov/centers/ames/research/technology-onepaggers/instrument_development.html)>
- Asner, G.P., Braswell, B.H., Schimel, D.S. and Wessman, C.A. 1998. Ecological research needs from multiangle remote sensing data. *Remote Sensing of Environment* 63, p. 155-165.
- Briottet, X., Hosgood, B., Meister, G., Sandmeier, S. and Serrot, G. 2004. Laboratory measurements of bi-directional reflectance. In Schönemark, M. von, Geiger, B. and Röser, H.P. (eds.), *Reflectance properties of vegetation and soil with a BRDF data base*, p. 173-194. Wissenschaft & Technik Verlag, Berlin.
- Brugge, C.J., Schaepman, M., Strub, G., Beisl, U., Demircan, A., Geiger, B., Painter, T.H., Paden, B.E. and Dozier, J. 2004. Field measurements of bi-directional reflectance. In Schönemark, M. von, Geiger, B. and Röser, H.P. (eds.), *Reflectance properties of vegetation and soil with a BRDF data base*, p. 195-224. Wissenschaft & Technik Verlag, Berlin.
- Clark, R.N., Swayze, G.A., Wise, R., Livo, K.E., Hoefen, T.M., Kokaly, R.F. and Sutley, S.J. 2003. USGS Digital Spectral Library splib05a. U.S. Geological Survey, Open File Report 03-395. Accessed online, July 2007 <<http://speclab.cr.usgs.gov/spectral-lib.html>>
- Hapke, B., DiMucci, D., Nelson, R. and Smythe, W. 1996. The cause of the hot spot in vegetation canopies and soils: Shadow-hiding versus coherent backscatter. *Remote Sensing of Environment* 58, p. 63-68.
- Jensen, J.R. 2007. *Remote sensing of the environment: An Earth resource perspective* (2nd ed.). Prentice Hall Series in Geographic Information Science, Upper Saddle River, New Jersey, 592 p.
- Lauer, D.T., Morain, S.A. and Salomonson, V.V. 1997. The Landsat program: Its origins, evolution, and impacts. *Photogrammetric Engineering & Remote Sensing* 63, p. 831-838.
- Lucht, W. 2004. Viewing the Earth from multiple angles: Global change and the science of multiangular reflectance. In Schönemark, M. von, Geiger, B. and Röser, H.P. (eds.), *Reflectance properties of vegetation and soil with a BRDF data base*, p. 9-29. Wissenschaft & Technik Verlag, Berlin.
- Lynch, D.K. and Livingston, W. 1995. *Color and light in nature*. Cambridge University Press, 254 p.
- Nilson, T. and Kuusk, A. 1989. A reflectance model for the homogeneous plant canopy and its inversion. *Remote Sensing of Environment* 27, p. 157-167.
- Ranson, K.J., Irons, J.R. and Williams, D.L. 1994. Multispectral bidirectional reflectance of northern forest canopies with the Advanced Solid-State Array Spectroradiometer (ASAS). *Remote Sensing of Environment* 47, p. 276-289.
- Schaaf, C.B. and Strahler, A.H. 1994. Validation of bidirectional and hemispherical reflectances from a geometric-optical model using ASAS imagery and pyranometer measurements of a spruce forest. *Remote Sensing of Environment* 49, p. 138-144.
- Schönemark, M. von, Geiger, B. and Röser, H.P. (eds.) 2004. *Reflectance properties of vegetation and soil with a BRDF data base*. Wissenschaft & Technik Verlag, Berlin, 352 p.